ELSEVIER

CrossMark

CHINESE
ASTRONOMY
AND ASTROPHYSICS

Chinese Astronomy and Astrophysics 48-2 (2024) 292–315

# Near-Earth Asteroids Orbit Determination by DRO Space-Based Optical Observations† ⋆

LIU Jia[1,2,3] SONG Ye-zhi[1△] HUANG Cheng-li[1,2,3] HU Xiao-gong[1]
TAN Long-yu[4]

[1] *Shanghai Astronomical Observatory, Chinese Academy of Sciences, Shanghai 200030*
[2] *School of Physical Science and Technology, Shanghai Tech University, Shanghai 201210*
[3] *School of Astronomy and Space Sciences, University of Chinese Academy of Sciences, Beijing 100049*
[4] *Shanghai Aerospace Control Technology Institute, Shanghai 201109*

**Abstract** In response to the problem that ground-based optical monitoring systems cannot monitor near-Earth asteroids which are in the direction too close to the Sun on the celestial sphere, we raise a method that tracks and determines the orbit of asteroids by Distant Retrograde Orbit (DRO) platforms with optical monitoring. Through data filtering by visibility analysis and the initial orbit information of the asteroids provided by Jet Propulsion Laboratory (JPL), the asteroids orbits are determined and compared with the reference orbit. Simulation results show that with a measurement accuracy of two arcseconds and an arc length of three years, the orbit determination accuracy of the DRO platform for near-Earth asteroids selected in the simulation example can reach tens of kilometers, especially the asteroids with Atira orbits to an accuracy of fewer than ten kilometers. In conclusion, the near-Earth asteroids monitoring systems based on DRO platforms are capable to provide sufficient monitoring effectiveness which enables precisely tracking of the target asteroids and forecast of their positions.

**Key words** minor planets—asteroids: near-Earth asteroids—spacecraft: distant retrograde orbit (DRO)satellite—celestial mechanics: orbit determination—methods: space-based optical monitoring—numerical

† Supported by the Key Cultivation Project of Shanghai Astronomical Observatory (Grant No.N20210601003) and the Civil Aerospace "14th Five-Year" Technology Pre-research Project (Grant No.KJSP2020020203)

Received 2022-09-27; revised version 2023-02-07

⋆ A translation of *Acta Astron. Sin.* Vol. 64, No. 6, pp. 66.1–66.18, 2023

△ syz@shao.ac.cn


PII:
10.1016/j.chinastron.2024.05.010

## 1. INTRODUCTION

The monitoring and research of asteroids have two main meanings. One is to prepare for the development and utilization of asteroid resources in the future[1, 2], and the other is to avoid the collision threat posed to the Earth by potentially dangerous asteroids[3]. There have been many asteroid impacts on the Earth in history: 65 million years ago, an asteroid with a diameter of about 10 km hit the Yucatan Peninsula in Mexico, which is believed to be an important cause for the extinction of the Earth's life, including dinosaurs[4]; in 1908, an asteroid impact event occurred in the Tunguska region of Russia, affecting an area of 2000 $km^2$; in 2013, an asteroid exploded after hitting Russia's Chelyabinsk region, injuring more than 1200 people[5]. By July 19, 2022, 29388 near-Earth asteroids have been discovered in the world, including 2291 potentially dangerous asteroids. To prevent and warn the threat of near-Earth asteroids impacting the Earth, countries around the world have carried out monitoring and warning of asteroids.

There are many ways to monitor and warn asteroids. According to the observation position, it can be divided into ground-based observation and space-based observation; according to the technical means, it can be divided into visible observation, infrared observation, and radar observation. At present, the ground-based large-aperture telescope is the main equipment for asteroid monitoring and early warning, which has the advantages of low construction cost, long operating distance, and mature method, but there is a blind area in the monitoring of the direction near the Sun, even if the monitoring ability is improved and the coverage is expanded, it is difficult to detect and warn in advance. The Chelyabinsk explosion was caused by the failure of ground-based telescopes to observe the asteroid in time. On March 15, 2020, an asteroid with a diameter of about 26 m approached the Earth from the sunward direction, only 328000 km away from the Earth, and was discovered two days after closest approach to the Earth; then on June 5, the Asteroid 2020 LD, also from the sunward direction, with a diameter of 89-200 m, flew by the 306675 km from the Earth, and was found two days after the closest approach to the Earth[6]. Compared with the ground-based optical monitoring system, the space-based optical monitoring system has a wide monitoring range and high observation accuracy, and it can meet the needs of continuous tracking and monitoring of targets, and can be used to make up for the shortcomings of ground-based observation equipment.

Low Earth Orbit (LEO), Sun-Earth system L1 point orbit, Venus-like orbit, Distant Retrograde Orbit (DRO), and Earth Pilot orbit are the main deployment orbits of space-based telescope platform. Shao et al.[7] proposed a plan to search for near-Earth asteroids with Venus-like orbits in 2015; civil organizations in the United States have proposed Sentinel Missions, planning to set the telescope in a Venus-like orbit. NEOCam (Near Earth Object Camera), a near-Earth object telescope in the United States, plans to launch a satellite into the L1 orbit of the Sun-Earth system in 2025 to monitor potentially dangerous asteroids near the Earth[8]. In 2012, Valsecchi et al.[9] first proposed to place a constellation consisted

of three satellites on DRO, but did not further evaluate its detection capability. Stramacchia et al.[10] analyzed the capabilities and characteristics of the monitoring constellation located on the orbit of the Sun-Earth System DRO.

Compared with foreign countries, China started later in the research on asteroid monitoring and early warning. In 2016, China proposed the NEA (Near-Earth Asteroid) Constellation of Heterogeneous Wide-field Near-Earth Object Surveyors (CROWN) scheme for deploying satellite constellations in Venus-like orbits[11]; in 2022, Li Mingtao's team and Zhao Haibin's team put forward the concept of space-based proximity warning mission for near-Earth asteroids in Earth's pilot orbit[6]; the Chang'e-2 lunar probe achieved China's first space-based exploration of an asteroid[12]; on April 24, 2022, China National Space Administration (CNSA) proposed to set up a near-Earth asteroid defense system, started to improve the establishment of ground-based and space-based asteroid monitoring and early warning systems, and carry out global cooperation to jointly respond to the threat of near-Earth asteroid impacts.

The Earth-Moon DRO is a retrograde resonant periodic orbit around the Moon. The spacecraft placed in this orbit can remain stable for a long time, and the long-term orbit maintenance only requires a low fuel cost. DRO has a moderate distance from the Earth and the Moon, can maintain continuous communication with the Earth, and is suitable for long-term isolated orbit missions such as deep space exploration, asteroid warning and protection. Bezrouk et al. studied the family of DRO orbits with stability up to 30 yr and suitable as parking orbits for the Earth-Moon system, and the stability of DRO orbits with amplitudes less than 50000 km from the center of the Moon and amplitudes at 60000–80000 km is very good[13]. Even if the orbit of DRO has a certain inclination with respect to the orbital plane of the Moon, the stability can reach tens of years.

For asteroids, accurate orbital elements can effectively and accurately predict the impact probability of asteroids. Therefore, to effectively carry out asteroid monitoring and early warning, the first step is to determine the orbit of the asteroid. In this paper, based on the optical measurement of near-Earth asteroids by the Earth-Moon DRO space-based platform, we gave the visibility conditions and orbit determination principle of the target celestial body. Through the simulation of optical angle measurement data, we determined the orbit of the target celestial body, compared the calculated orbit with the reference orbit, and analyzed the orbit determination performance of the DRO platform for four different types of near-Earth asteroids.

## 2. EARTH-MOON DRO ORBIT

The circular restricted three-body problem is a common model to study the orbit of the Earth and the Moon. The two main celestial bodies, the Earth $m_1$ and the Moon $m_2$, are regarded as mass points and move in a circle around the common center of mass. The third body spacecraft is affected by the gravitation of the two main celestial bodies, but does

not affect the motion of the two main celestial bodies. We used the center of mass rotating coordinate system $X$-$Y$-$Z$ to describe the circular restricted three-body problem, with the center of mass of the Earth-Moon system as the origin of the coordinate system, the $X$ axis pointing from the center of the Earth to the center of the Moon, and the $Z$ axis taking the direction of the Earth-Moon orbit. Then, we introduced the mass parameter $\mu_m = \frac{m_2}{m_1+m_2}$ to characterize the circular restricted three-body problem. The Earth and the Moon are located at $-\mu_m$ and $1-\mu_m$, respectively. Reference [14] gives the dynamical equations of the spacecraft in this system.

Hill's restricted three-body problem is a special circular restricted three-body problem for systems with small values of $\mu_m$ and spacecraft orbits close to smaller primary bodies[10]. When $\mu_m = 0$, the circular restrictive three-body problem can be reduced to a Kepler model in a rotational coordinate system. Hénon[15] proposed to simplify the system of equations considering that $\mu_m$ is approaching 0. Unlike the center-of-mass rotational coordinate system used in the circular restricted three-body problem, the Hill's problem uses the synodic coordinate system $\xi-\eta-\zeta$, with the Moon as the origin of the coordinate system, and the Earth in the negative direction of the $\xi$ axis. Fig. 1 shows the coordinate systems used for the circular restricted three-body problem and the Hill's problem.

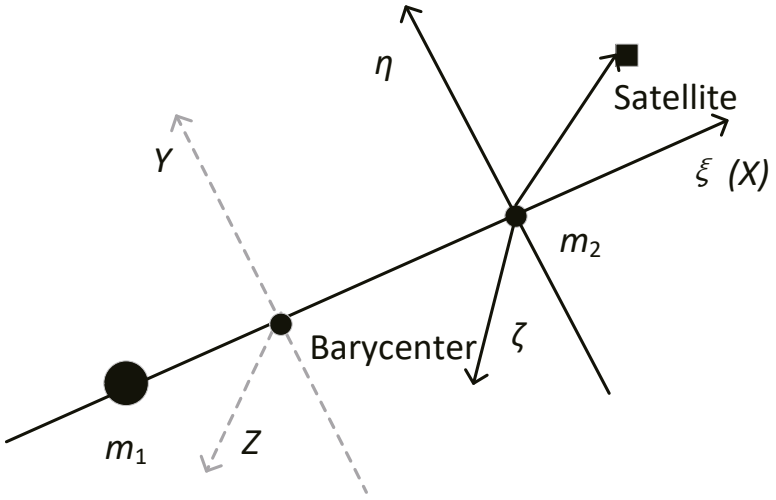


Fig. 1 Coordinate systems for planar circular restricted three-body problem and Hill's problem

In the Hill's problem, the equation of motion of the third body spacecraft is:

$$\begin{cases} \ddot{\xi} - 2\dot{\eta} - 3\xi = \dfrac{\partial W}{\partial \xi}, \\ \ddot{\eta} + 2\dot{\xi} = \dfrac{\partial W}{\partial \eta}, \\ \ddot{\zeta} + \zeta = \dfrac{\partial W}{\partial \zeta}, \end{cases} \tag{1}$$

where $W = \frac{1}{\sqrt{\xi^2+\eta^2+\zeta^2}}$, and the Jacobi's integral in Hill's system is:

$$\Gamma = 3\xi^2 + \zeta^2 + \frac{2}{\sqrt{\xi^2+\eta^2+\zeta^2}} - \left(\dot{\xi}^2 + \dot{\eta}^2 + \dot{\zeta}^2\right) . \tag{2}$$

Hénon et al.[15] classified the periodic orbits in the circular restricted three-body problem into family f, family g, family a, and family c. DRO orbit family belongs to family f, which is a special plane symmetric orbit family in the circular restricted three-body problem, and has Lyapunov stability. The DRO of the Earth-Moon system is retrograde around the Moon, with good coverage of the Earth and the Moon and stable orbit, so it is suitable for long-term missions in deep space. Reference [14] studied the dynamic system structure around the orbit family of DRO with the circular restricted three-body problem as the dynamic model; Reference [16] studied the design method of DRO with the Earth-Moon as the background, and analyzed the orbit characteristics and main perturbation factors of the retrograde periodic orbit of the Earth-Moon DRO under the actual force environment. The amplitude range of DRO orbit is large. When the amplitude is small, the DRO can be regarded as a circumlunar orbit in a low orbit, with the Moon as the central celestial body, and the Earth's gravity as the perturbative force. However, for the large amplitude DRO, the influence of the Earth is significant, and the classical orbital elements are no longer applicable, which has been studied in Reference [17]. In the orbit design of DRO in this paper, we considered the complete mechanical model and used the numerical method to calculate. In the rotational coordinate system with the center of the Moon as the origin, the initial $X$ amplitude of DRO was used to represent the size of DRO. In this study, we selected a stable orbit with an initial $X$ amplitude of 30000 km in the DRO orbit family to place a satellite to monitor near-Earth asteroids.

## 3. VISIBILITY ANALYSIS OF NEAR-EARTH ASTEROIDS

### 3.1 Optical Geometry Constraints

When a space-based platform satellite observes near-Earth asteroids, it is disturbed by light sources such as sunlight, Aurora, radiation from the Earth's edge, reflected light from other celestial bodies, and starlight, among which sunlight is the main disturbing factor. When a platform satellite observes a near-Earth object against sunlight, it will be unable to observe the target because the background light is too strong. The angle between the target-platform-sun is defined as $\theta_{\min}$, and the optical geometry constraints of the simulated screening data are shown in Fig. 2.

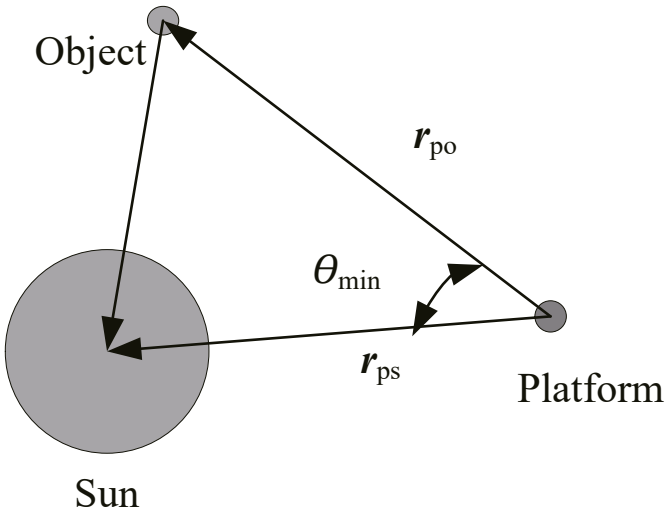


Fig. 2 Optical geometry constraints

During the simulation observation in this study, we set the observable condition as the target celestial body can be observed only when $\theta_{\min}$ is greater than 40°, that is:

$$\theta_{\min} = \arccos\left(\frac{\boldsymbol{r}_{\mathrm{po}}}{|\boldsymbol{r}_{\mathrm{po}}|} \cdot \frac{\boldsymbol{r}_{\mathrm{ps}}}{|\boldsymbol{r}_{\mathrm{ps}}|}\right) > 40^{\circ}\,. \tag{3}$$

### 3.2 Spatial Geometry Constraints

When the observation platform observes the target celestial body, it may be blocked by the Earth, Mars, Moon, and other celestial bodies, resulting in the platform can not observe the target or the observation accuracy is poor. Taking the Earth blocking as an example, the spatial geometry relationship between the observation platform and the target celestial body is shown in Fig. 3.

$$\arccos\left(-\frac{\boldsymbol{\rho}}{|\boldsymbol{\rho}|} \cdot \frac{\boldsymbol{r}_{\mathrm{pe}}}{\boldsymbol{r}_{\mathrm{pe}}}\right) > \arcsin\left(\frac{R_{\mathrm{e}} + h}{|\boldsymbol{r}_{\mathrm{pe}}|}\right)\,, \tag{4}$$

where $\boldsymbol{\rho}$ is the gaze vector, $\boldsymbol{r}_{\mathrm{pe}}$ denotes the position vector of the observation platform relative to the Earth, $R_{\mathrm{e}}$ is the radius of the Earth, and $h$ is the height of the atmosphere.

In addition, the observation of the target celestial body will also be constrained by the field of view conditions of the observation equipment itself and the performance conditions such as the limiting apparent magnitude of the detectable target. In the study of asteroid visibility in this paper, we only considered the constraints of optical geometry and spatial geometry, and did not consider the brightness visibility and other constraints related to the camera design for the time being.

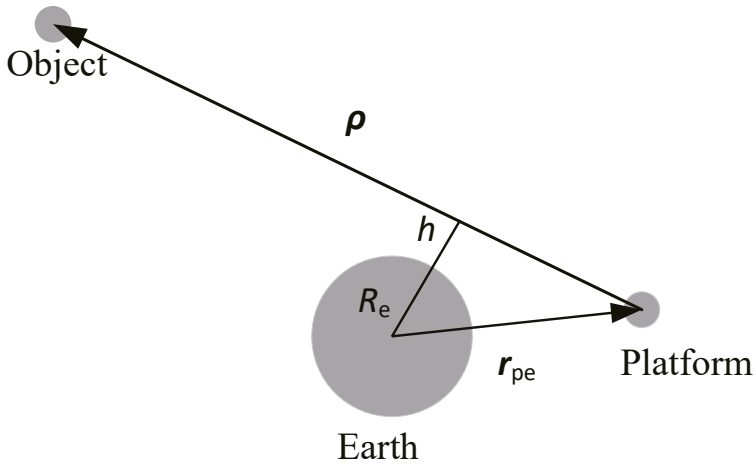


Fig. 3 Spatial geometry constraints

## 4. PRINCIPLE OF SPACE-BASED OPTICAL ORBIT DETERMINATION

The equation of motion of a near-Earth object (NEO) around the Sun is:

$$\begin{cases} \ddot{\boldsymbol{r}} = -\dfrac{\mu}{r^3}\boldsymbol{r} + \boldsymbol{F}_\varepsilon(\boldsymbol{r}, \dot{\boldsymbol{r}}, t; \boldsymbol{p}) \,, \\ t_0 : \boldsymbol{r_0} = \boldsymbol{r}(t_0), \boldsymbol{r_0} = \dot{\boldsymbol{r}}(t_0) \,, \end{cases} \tag{5}$$

where $\mu = GM_c$ is the gravitational constant of the central celestial body, $G$ is the gravitational constant, $M_c$ is the mass of the central celestial body; $\boldsymbol{F}_\varepsilon$ is the perturbative force (most of the orbits of NEOs are located between the Earth and Mars, so the considered perturbations are mainly the gravitational perturbations of other celestial bodies and post-Newtonian effects); $\boldsymbol{r}$ and $\dot{\boldsymbol{r}}$ are respectively position and velocity vectors; $\boldsymbol{p}$ is the kinetic parameter; $t_0$ is the initial epoch, $\boldsymbol{r_0}$ denotes the position vector of the target object at time $t_0$.

In this paper, based on the dynamic orbit determination method, we improved the orbits of near-Earth asteroids. In the orbit improvement, the orbit parameters to be solved of the target celestial body are called the state quantity $\boldsymbol{X}$, $\boldsymbol{F}(\boldsymbol{X}, t)$ is the mechanical parameter and velocity related to the state quantity, $\boldsymbol{X}_0$ is the state quantity to be estimated and satisfies the following state differential equation:

$$\begin{cases} \dot{\boldsymbol{X}} = \boldsymbol{F}(\boldsymbol{X}, t) \,, \\ t_0 : \boldsymbol{X}|_{t_0} = \boldsymbol{X}_0 \,. \end{cases} \tag{6}$$

The optical angle measurement data (right ascension and declination) of the satellite platform is recorded as the observational quantity $\boldsymbol{Y}_j$, and the observation equation it

satisfies is as follows:

$$\boldsymbol{Y}_j = \boldsymbol{G}(\boldsymbol{X}_j, t_j) + \boldsymbol{\varepsilon}_j \,, \tag{7}$$

where $\boldsymbol{Y}_j$ is a set of the observational quantity at time $t_j$, $j$ is a subscript at a certain time; $\boldsymbol{G}$ is the theoretical value of the corresponding observational quantity; $\boldsymbol{X}_j$ is the state vector of target celestial body at time $t_j$; $\boldsymbol{\varepsilon}_j$ is the measurement error at time $t_j$.

The observation equation and the state equation were linearized to obtain the basic equation for precise orbit determination[18]:

$$\begin{cases} \boldsymbol{y} = \boldsymbol{H}\Delta\boldsymbol{X} + \boldsymbol{\varepsilon} \,, \\ \boldsymbol{H} = \left( \dfrac{\partial \boldsymbol{G}}{\partial \boldsymbol{X}} \dfrac{\partial \boldsymbol{X}}{\partial \boldsymbol{X_0}} \right)_{\boldsymbol{X}=\boldsymbol{X}^*} \,, \\ \Delta\boldsymbol{X} = \boldsymbol{X}_0 - \boldsymbol{X}_0^* \,, \end{cases} \tag{8}$$

where $\boldsymbol{y}$ is the residual error, which is the difference between the observed value and the theoretical value; $\Delta\boldsymbol{X}$ is the corrected value of the state quantity to be estimated; $\boldsymbol{\varepsilon}$ is the measurement error; $\frac{\partial \boldsymbol{X}}{\partial \boldsymbol{X}_0}$ is the state transition matrix, which is the partial derivative of the target current state vector to the initial state vector, usually represented by $\boldsymbol{\Phi}(t, t_0)$; $\boldsymbol{X}^*$ is the reference state quantity at a certain time; $\boldsymbol{X}_0^*$ is the reference state quantity of the initial epoch.

The principle of precise orbit determination is to give a set of initial quantities $\boldsymbol{X}_0^*$, use a large number of observation data, solve Equation (8), obtain the corrected value of the state quantity to be estimated, and then obtain the improved state quantity, substitute the improved state quantity as the estimated quantity again, and calculate iteratively to obtain the target orbit solution that meets the accuracy.

The orbit determination strategy for near-Earth asteroids is shown in Table 1, where Q in QR represents orthogonal matrix and R stands for upper triangular matrix; KSG is an abbreviation for the Inventor of the integrator, Krogh Shampine Gordon.

**Table 1 Strategy for the orbit determination**

| Category | Description |
|---|---|
| Reference Frames | J2000.0 Celestial Reference System |
| N-body Perturbation | DE405 Planetary Ephemeris |
| General Relativity | Parametric Post-Newtonian Formalism |
| Parameter Estimation Method | Least Square Batch Processing Based on QR Decomposition |
| Outlier Elimination | 3 $\sigma$ Criterion |
| Integrator | KSG Integrator |

## 5. ORBIT DETERMINATION SIMULATION TEST

In this study, we selected four asteroids with different orbital types to determine their orbits. Table 2 shows the orbital elements of the four asteroids in the heliocentric ecliptic inertial system provided by NASA's Jet Propulsion Laboratory (JPL), where $a$ is the orbit semi-major axis, $e$ is the orbital eccentricity, $i$ is the orbital inclination, $\Omega$ is the right ascension of the ascending node, $\omega$ is the argument of perihelion, and $M$ is the mean anomaly. According to the simulation conditions, the angle measurement accuracy was 2 arcseconds, the data sampling interval was 1 h, the near-Earth asteroids were observed, and the observation data were generated by simulation. This simulation condition considered the constraints of the optical geometry and space geometry described in Section 3. In practical engineering, the available measurement data are also constrained by the working mode of the camera and the load on the satellite.

**Table 2 Orbital elements of near-Earth asteroids**

| Asteroids | Type | Epoch[a] | $a$/au | $e$ | $i/^\circ$ | $\Omega/^\circ$ | $\omega/^\circ$ | $M/^\circ$ |
|---|---|---|---|---|---|---|---|---|
| 1996 HW1 | Amor | 2014-04-07 | 2.046 | 0.449 | 8.437 | 177.171 | 177.063 | 324.180 |
| 1951 RA | Apollo | 2011-07-28 | 1.246 | 0.335 | 13.337 | 337.258 | 276.806 | 104.715 |
| 2013 JX28 | Atira | 2013-12-08 | 0.601 | 0.564 | 10.767 | 39.992 | 354.848 | 257.287 |
| 1998 TU3 | Aten | 2014-04-15 | 0.787 | 0.484 | 5.413 | 102.209 | 84.674 | 215.513 |

[a] The time is 00:00:00.00

### 5.1 Observing Asteroid 1996 HW1 by DRO Platform

Asteroid 1996 HW1 is a near-Earth asteroid with an orbital type of Amor discovered by the Kitt Peak Observatory during the space monitoring program on April 23, 1996, and its orbital period is 2.93 yr.

The orbit determination selected the arc section from 0:00 on April 7, 2014 to 0:00 on April 7, 2017. According to the simulation conditions, the observation data were generated by simulation, and the observation data were used to track and determine the orbit. The single-platform observation residual of the orbit determination arc for 3 yr is shown in Figure 4. In the figure, POD means precise orbit determination.

The upper part of Fig. 4 is the right ascension residual of the single DRO platform observation data, and the lower part is the declination residual of the observation data, with the abscissa being the observation time (Universal Time Coordinated, UTC) and the ordinate being the residual range. Fig. 5 shows the comparison results of the single DRO tracking for orbit determination of Asteroid 1996 HW1 and the simulated orbit in RTN coordinate system, where R is the radial direction, T is the trace direction, N is the normal direction of the orbit plane, and RMS is the root mean square deviation. Fig. 5(a) is the deviation of the position, and Fig. 5(b) is the deviation of the velocity. The horizontal axis

is the observation time, and the vertical axis is the deviation range. The orbit accuracy is about 30 km magnitude. Fig. 6 shows the residuals of Asteroid 1996 HW1 observed by the dual DRO platform under the same simulation conditions. In Fig. 6, the upper figure shows the observation residuals of platform 1, and the lower figure shows the observation residuals of platform 2 (the same for the subsequent residual figures).

Fig. 7 shows the comparison result between the orbit obtained by tracking for orbit determination of Asteroid 1996 HW1 by dual DRO and the simulated orbit in RTN coordinate system, and the orbit accuracy is about 30 km.

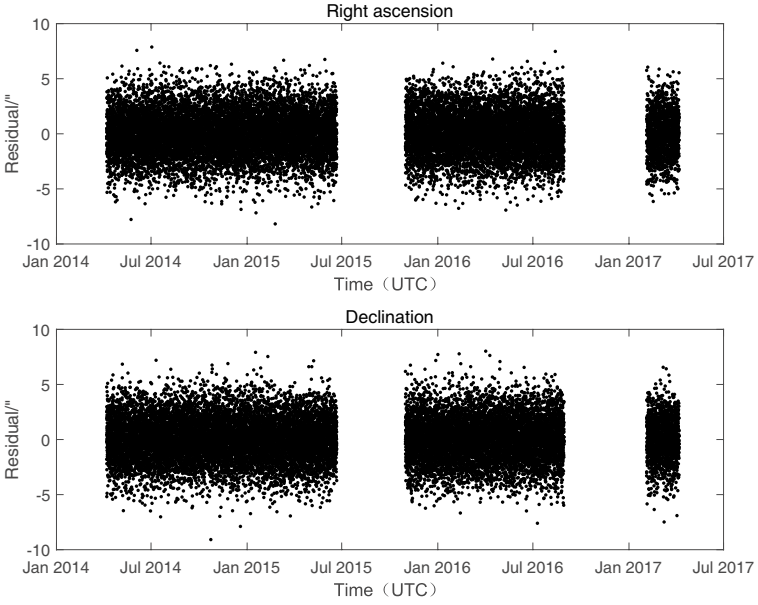


Fig. 4 3-year POD residuals of single DRO on Asteroid 1996 HW1

### 5.2 Observing Asteroid 1951 RA by DRO Platform

Asteroid 1951 RA is a potentially dangerous Apollo type asteroid discovered in Palomar on September 14, 1951, with an orbital period of 1.39 yr. The orbit determination selected the arc section from 0:00 on July 28, 2011 to 0:00 on July 28, 2014.

According to the simulation conditions, the observation data were generated by simulation, and the observation data were used to track and determine the orbit. The single-platform observation residual of the orbit determination arc for 3 yr is shown in Fig. 8.

Fig. 9 shows the comparison results of the orbit determination of Asteroid 1951 RA by single DRO and the simulated orbit in the RTN coordinate system, and the orbit determination accuracy is about 100 km. Fig. 10 shows the residuals of Asteroid 1951 RA observed by the dual DRO platform under the same simulation conditions.

Fig. 11 shows the comparison result between the orbit obtained by tracking for orbit determination of Asteroid 1951 RA by dual DRO and the simulation orbit in RTN coordinate

system, and the orbit accuracy is about 20 km.

### 5.3 Observing Asteroid 2013 JX28 by DRO Platform

Asteroid 2013 JX28, first discovered in 2016, is an Atira-type near-Earth asteroid with an orbital period of 0.47 yr. The orbit determination selected the arc section from 0:00 on December 8, 2013 to 0:00 on December 8, 2016.

According to the simulation conditions, the observation data were generated by simulation, and the observation data were used to track and determine the orbit. The single-platform observation residual of the orbit determination arc for 3 yr is shown in Fig. 12.

Fig. 13 shows the comparison results of the orbit determination of 2013 JX28 by single DRO and the simulated orbit in the RTN coordinate system, and the orbit determination accuracy is about 28 km. Fig. 14 shows the residuals of 2013 JX28 observed by the dual DRO platform under the same simulation conditions.

Fig. 15 shows the comparison result between the orbit obtained by tracking for orbit determination of Asteroid 2013 JX28 by dual DRO and the simulation orbit in RTN coordinate system, and the orbit accuracy is about 9 km.

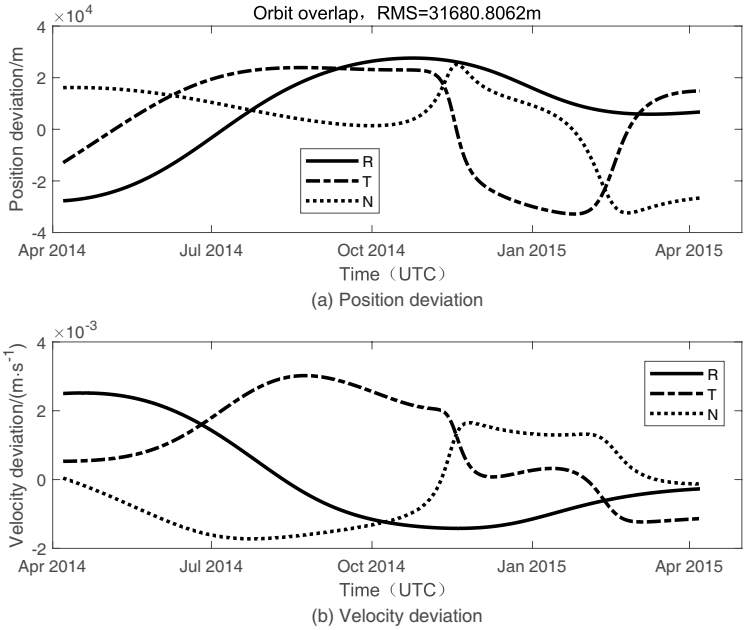


Fig. 5 Comparison between orbit determination and simulated orbit of single DRO on Asteroid 1996 HW1

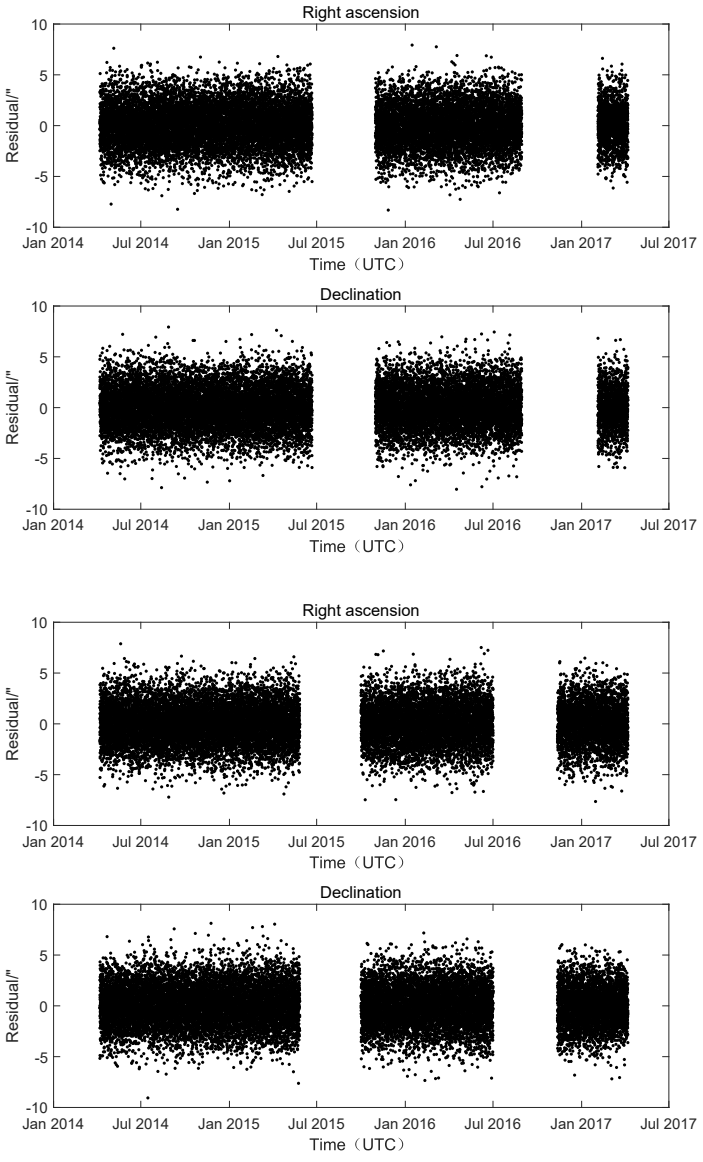


Fig. 6 3-year POD residuals of dual DRO on Asteroid 1996 HW1

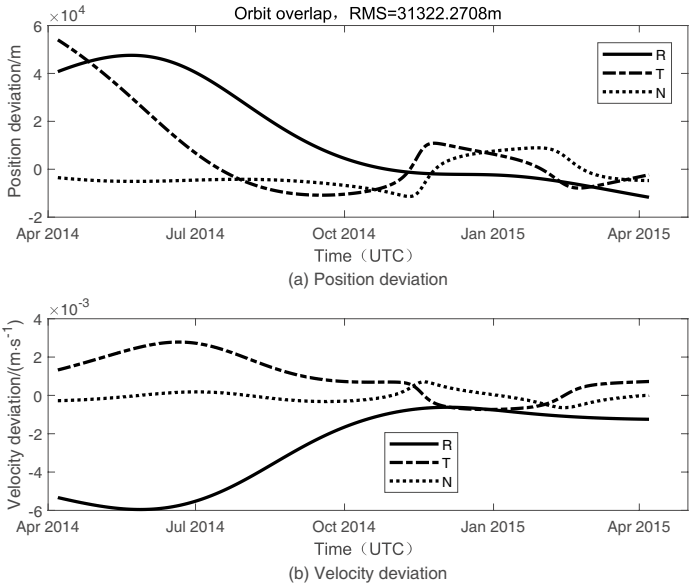


Fig. 7 Comparison between orbit determination and simulated orbit of dual DRO on Asteroid 1996 HW1

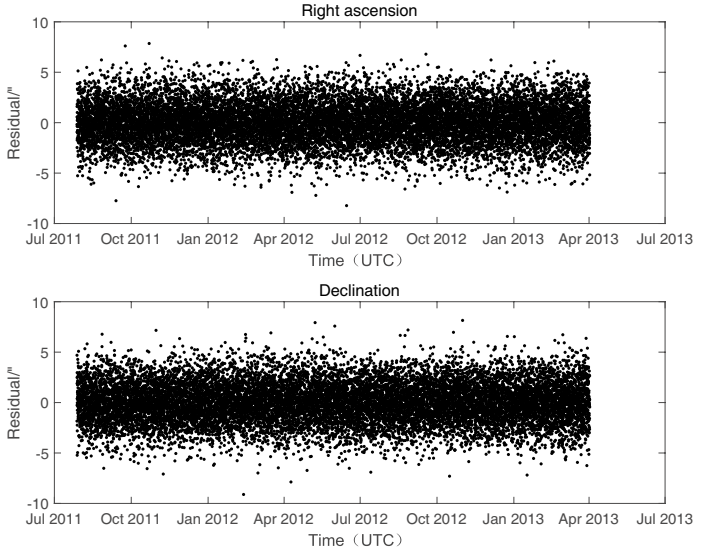


Fig. 8 3-year POD residuals of single DRO on Asteroid 1951 RA

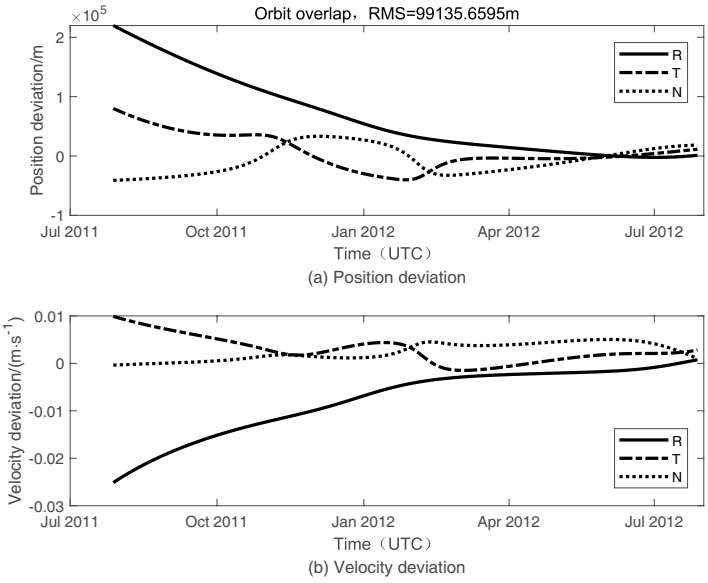


Fig. 9 Comparison between orbit determination and simulated orbit of single DRO on Asteroid 1951 RA

### 5.4 Observing Asteroid 1998 TU3 by DRO Platform

Asteroid 1998 TU3, discovered by LINEAR on October 13, 1998, is a near-Earth asteroid with an orbital type of Aten and an orbital period of 0.7 yr. The orbit determination selected the arc section from 0:00 on April 15, 2014 to 0:00 on April 15, 2017.

According to the simulation conditions, the observation data were generated by simulation, and the observation data were used to track and determine the orbit. The single-platform observation residual of the orbit determination arc for 3 yr is shown in Fig. 16.

Fig. 17 shows the comparison results of the orbit determination of Asteroid 1998 TU3 by single DRO and the simulated orbit in the RTN coordinate system, and the orbit determination accuracy is about 46 km. Fig. 18 shows the residuals of Asteroid 1998 TU3 observed by the dual DRO platform under the same simulation conditions.

Fig. 19 shows the comparison result between the orbit obtained by tracking for orbit determination of Asteroid 1998 TU3 by dual DRO and the simulation orbit in RTN coordinate system, and the orbit accuracy is about 29 km.

Based on the above simulation results, when the angle measurement accuracy is 2 arcseconds, the data sampling interval is 1 h, and the orbit determination arc length is 3 yr, the orbits of asteroids with different orbit types are determined by the single DRO space-based platform and the dual DRO space-based platform. The residuals of each observatory and station in different simulation examples are roughly equivalent to the simulated noise. The comparison of orbit determination results is shown in Table 3.

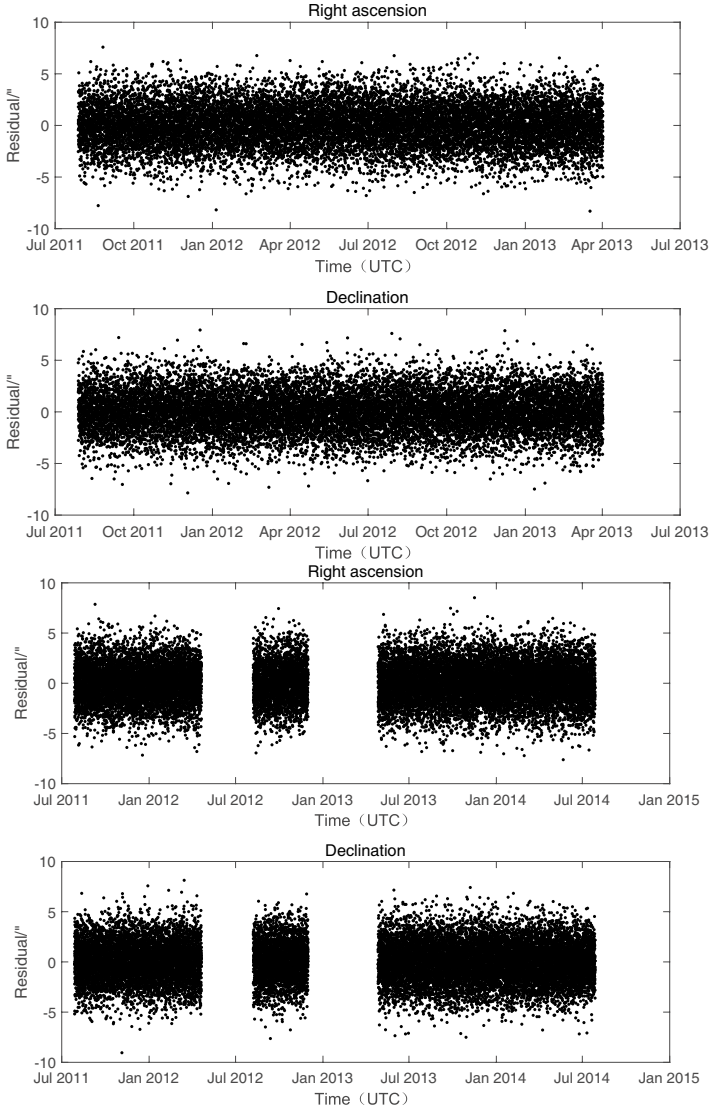


Fig. 10 3-year POD residuals of dual DRO on Asteroid 1951 RA

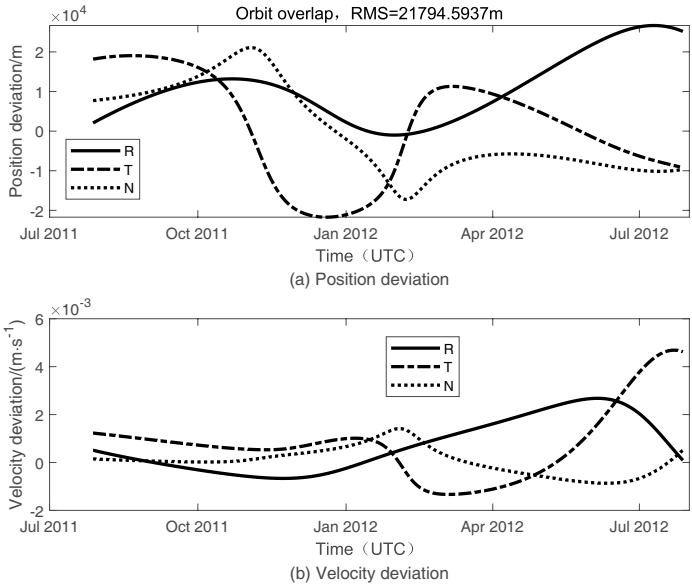


Fig. 11 Comparison between orbit determination and simulated orbit of dual DRO on Asteroid 1951 RA

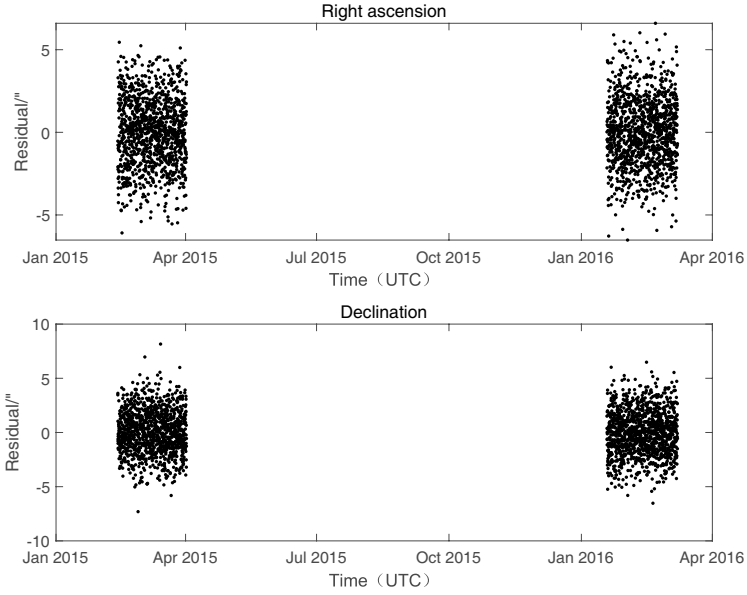


Fig. 12 3-year POD residuals of single DRO on Asteroid 2013 JX28

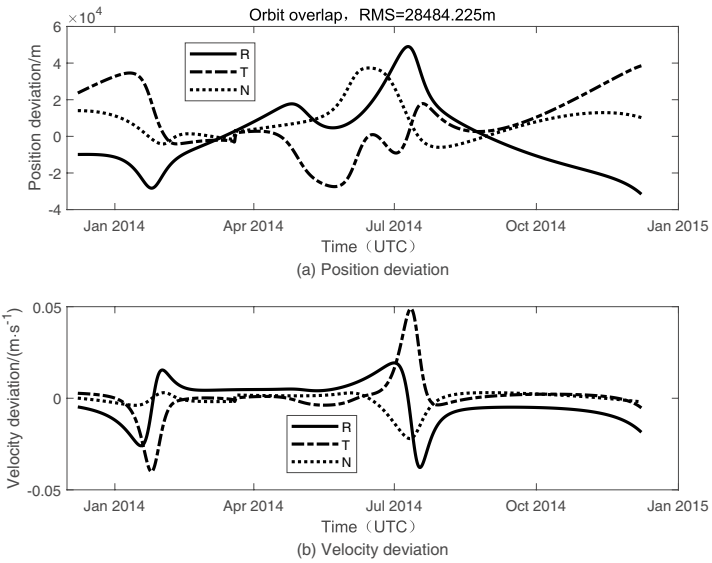


Fig. 13 Comparison between orbit determination and simulated orbit of single DRO on Asteroid 2013 JX28

**Table 3 POD results statistics with 1 h data sampling interval**

| Asteroids | Type | $\sigma_1^{\mathrm{a}}$/km | $\sigma_2^{\mathrm{b}}$/km |
|---|---|---|---|
| 1996 HW1 | Amor | 31.681 | 31.322 |
| 1951 RA | Apollo | 99.136 | 21.795 |
| 2013 JX28 | Atira | 28.484 | 8.840 |
| 1998 TU3 | Aten | 46.237 | 29.346 |

[a] the orbit determination accuracy of the single DRO platform

[b] the orbit determination accuracy of the dual DRO platform

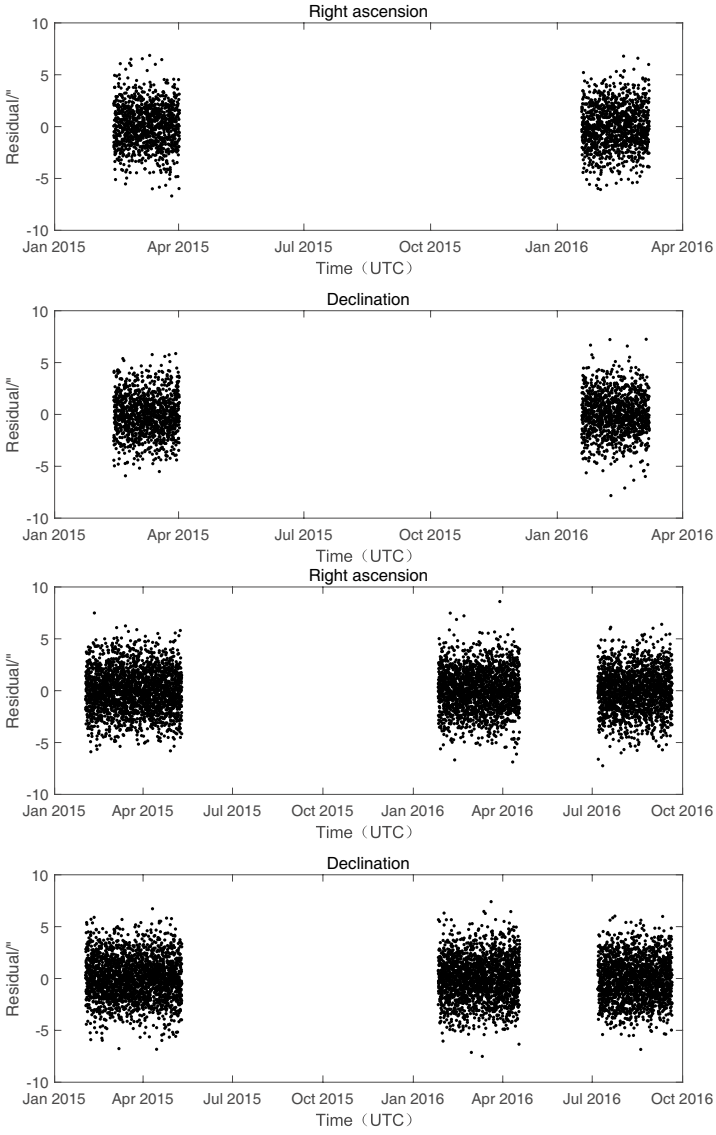


Fig. 14 3-year POD residuals of dual DRO on Asteroid 2013 JX28

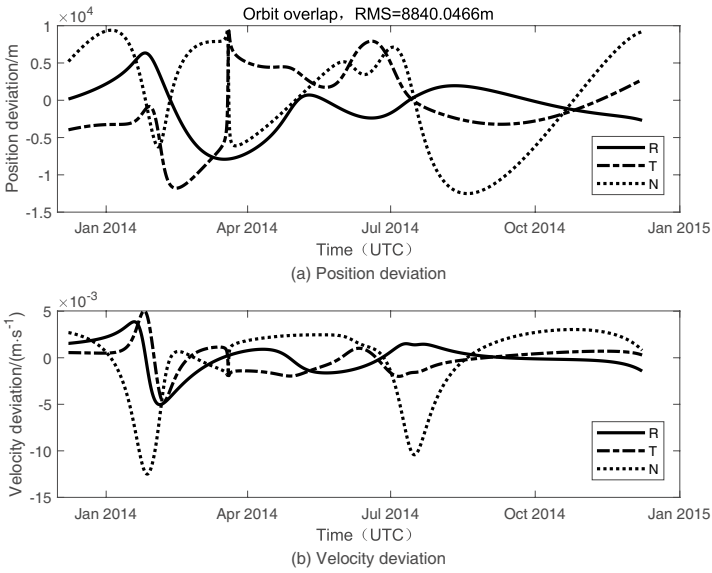


Fig. 15 Comparison between orbit determination and simulated orbit of dual DRO on Asteroid 2013 JX28

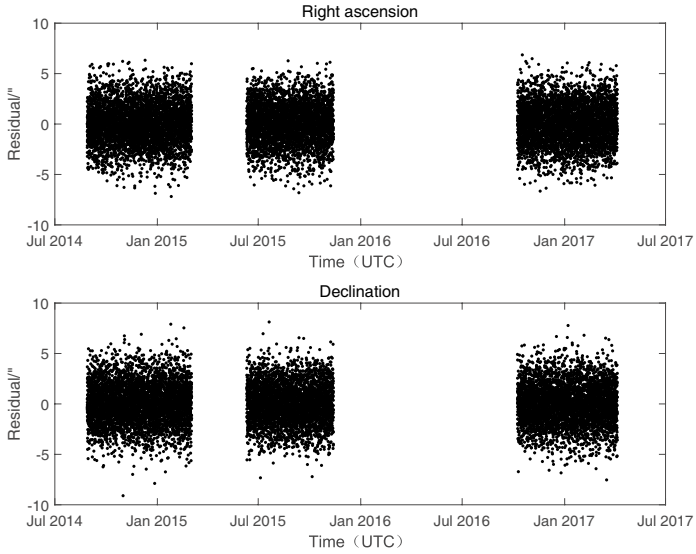


Fig. 16 3-year POD residuals of single DRO on Asteroid 1998 TU3

As shown in Table 3, for the Amor type Asteroid 1996 HW1, there is no significant difference between the single-DRO orbit determination accuracy and the dual-DRO orbit determination accuracy, both of which are about 30 km; for Apollo type Asteroid 1951 RA and Aten type Asteroid 1998 TU3, when the number of DRO space-based platforms is increased from one to two, the orbit determination accuracy is improved significantly and

can be up to 30 km; the orbit determination accuracy of Atria type Asteroid 2013 JX28 is the highest, and the orbit determination accuracy of dual DRO can be within 10 km, which meets the general orbit monitoring requirements. The main reason why the orbit determination accuracy of the four types of asteroids by the DRO space-based platform is different is that the observation geometry of the near-Earth Asteroids with different orbit types is different from that constructed by the observation platform. Besides, due to the different periods of motion of different asteroids, the proportion of the observed arc length to the whole orbit is also different. In this paper, four different types of asteroid orbits we selected for calculation and analysis are representative, and can be used as a preliminary reference for related tasks. In the specific engineering, there will be some differences in the accuracy of orbit determination of different asteroids. In this study, we also set the data sampling interval at 0.5 h. Under the simulation conditions of the same angle measurement accuracy and orbit determination arc length, the orbit determination accuracy of single DRO space-based platform and dual DRO space-based platform for asteroids with different orbit types is shown in Table 4.

From Tables 3 and 4, we can see that the sampling interval will affect the orbit determination accuracy of near-Earth Asteroids. Under the same observation arc length, the shorter the sampling interval is, the more observation data are obtained, and the better the orbit determination accuracy is. However, in the case of long-term observation, if the observation arc is long enough, the sampling interval will not have a significant impact on the orbit determination accuracy. Therefore, in some cases, reducing the sampling interval can improve the accuracy of orbit determination.

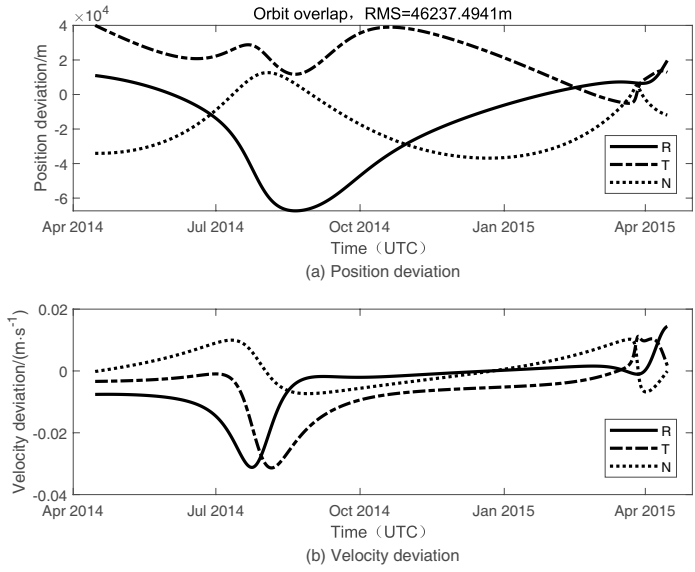


Fig. 17 Comparison between orbit determination and simulated orbit of single DRO on Asteroid 1998 TU3

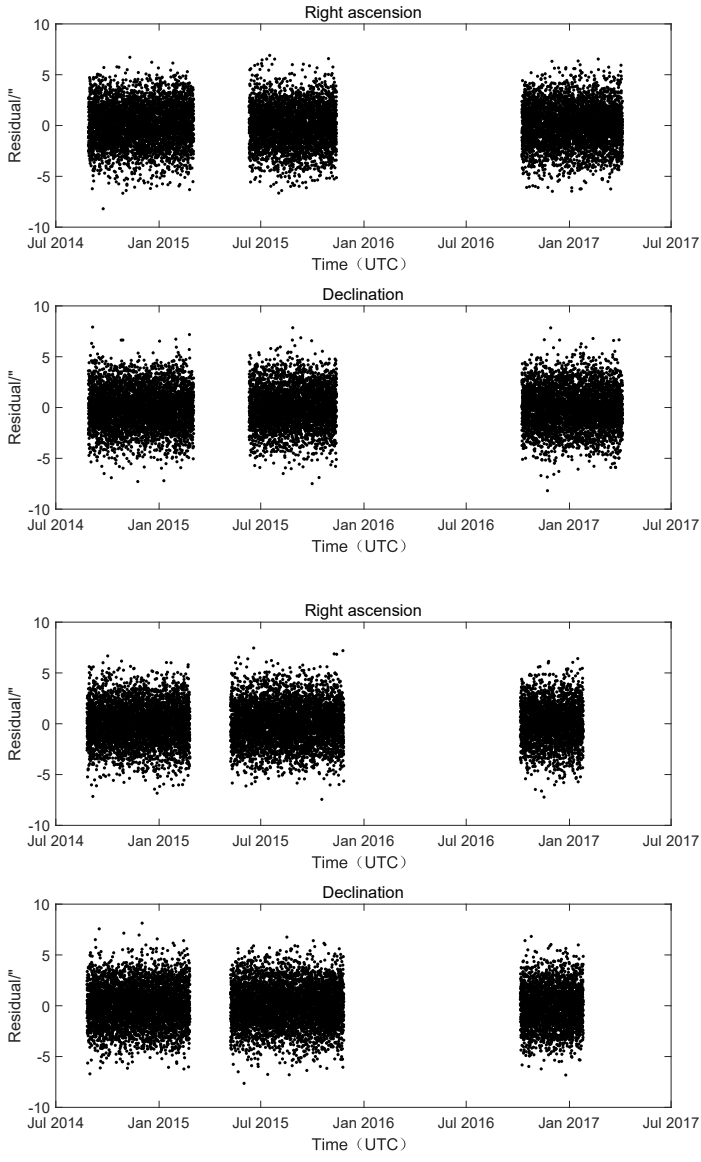


Fig. 18 3-year POD residuals of dual DRO on Asteroid 1998 TU3

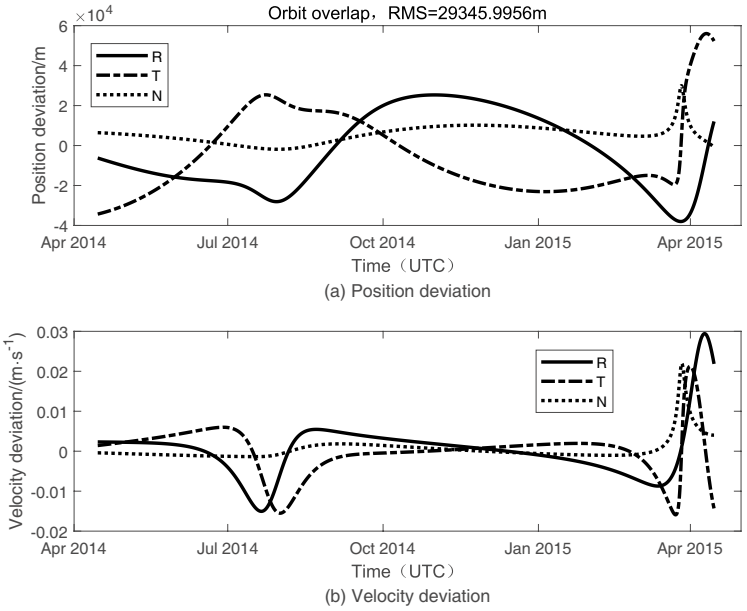


Fig. 19 Comparison between orbit determination and simulated orbit of dual DRO on Asteroid 1998 TU3

**Table 4 POD results statistics with data sampling interval of 0.5 h**

| Asteroids | Type | $\sigma_1$/km | $\sigma_2$/km |
|---|---|---|---|
| 1996 HW1 | Amor | 26.962 | 22.175 |
| 1951 RA | Apollo | 30.440 | 13.095 |
| 2013 JX28 | Atira | 27.160 | 4.340 |
| 1998 TU3 | Aten | 22.309 | 20.754 |

## 6. CONCLUSIONS

In response to the problem of blind spots in ground-based tracking observation of near-Earth asteroids, we proposed a method for determining the orbits of near-Earth asteroids by Earth-Moon DRO space-based optical measurements. Through optical visibility analysis, we screened the simulated observation data, and used the initial orbit information of asteroids provided by JPL to determine the orbit by numerical method.

For different orbit types of near-Earth asteroids, when the data sampling interval is 1 h and the measurement noise is 2 arcseconds, the orbit determination accuracy of the target celestial body by DRO is different. Increasing the number of DRO observation platforms can effectively improve the orbit determination accuracy of Apollo, Atira, and Aten types of asteroids, and the orbit determination accuracy of Atira type asteroids is the best and can

be within 10 km. In addition, the sampling interval will also affect the orbit determination accuracy, and reducing the sampling interval can improve the orbit determination accuracy.

The Earth-Moon DRO platform can effectively make up for the blind area of the ground-based optical monitoring system. Through optimizing the deployment, the early warning of near-Earth asteroids from the sun direction can be realized for a longer time, which has certain significance for the cataloguing, monitoring, and early warning of asteroids.

**ACKNOWLEDGEMENTS** We would like to thank the International Minor Planet Center for providing the online data download service and the JPL/Horizons system for providing the online calendar service.

## References


1 Hein A. M., Matheson R., Fries D., AcAau, 2020, 168, 104

2 Sonter M. J., AcAau, 1997, 41, 637

3 Billings L., SpPol, 2015, 33, 8

4 Yang Z. G., Lin Q., Science Advances, 2007, 53, 12

5 Borovička J., Spurný P., Brown P., et al., Nature, 2013, 503, 235

6 Wang X., Zheng J., Li M., et al., Icarus, 2022, 377, 114906

7 Shao M., Turyshev S. G., Spangelo S., et al., A&A, 2017, 603, A126

8 Sun H. B., Sun S. L., Journal of Deep Space Exploration, 2020, 7, 197

9 Valsecchi G. B., Perozzi E., Rossi A., Proceedings of the International Astronomical Union, 2012, 16, 488

10 Stramacchia M., Colombo C., Bernelli-Zazzera F., AdSpR, 2016, 58, 967

11 Wu W. R., Gong Z. Z., Tang Y. H., et al., Strategic Study of CAE, 2022, 24, 140

12 Cao J. F., Hu S. J., Liu L., et al., Journal of Beijing University of Aeronautics and Astronautics, 2014, 40, 1095

13 Bezrouk C., Parker J. S., Ap&SS, 2017, 362, 176

14 Chen G. H., Yang C. H., Zhang C., et al., Journal of Beijing University of Aeronautics and Astronautics, 2022, 48, 2576

15 Hénon M., A&A, 1969, 9, 24

16 Wu X. J., Zeng L. C., Gong Y. K., Journal of Beijing University of Aeronautics and Astronautics, 2020, 46, 883

17 Xu M., Xu S. J., Journal of Astronautics, 2009, 30, 1785

18 Liu L., Orbit Theory of Spacecraft, Beijing: National Defense Industry Press, 2000